HTLV-1 bZIP Factor Suppresses Apoptosis by Attenuating the Function of FoxO3a and Altering its Localization

Azusa Tanaka-Nakanishi[1], Jun-ichirou Yasunaga[1] Ken Takai[1], and Masao Matsuoka[1*]

1 *Laboratory of Virus Control, Institute for Virus Research, Kyoto University, 53 Shogoin Kawahara-cho, Sakyo-ku, Kyoto 606-8507, Japan*

Running title: HBZ Mediated Inhibition of Apoptosis

Keywords: HTLV-1, HBZ, Apoptosis, FoxO3a, Bim

[*]Corresponding author. Mailing address for M. Matsuoka: Institute for Virus Research, Kyoto University, 53 Shogoin Kawahara-cho, Sakyo-ku, Kyoto 606-8507, Japan. Phone: +81-75-751-4048, FAX: +81-75-751-4049.

E-mail: mmatsuok@virus.kyoto-u.ac.jp

Word count for text: 5726

Total number of figures and tables: 5 figures and 1 table

Disclosure of Potential Conflicts of Interest

The authors have declared that no competing interests exist.

Abstract

As the infectious agent causing human adult T cell leukemia (ATL), the HTLV-1 virus spreads in vivo primarily by cell-to-cell transmission. However, the factors that determine its transmission efficiency are not fully understood. The viral genome encodes the HTLV-1 bZIP factor (HBZ) which is expressed in all ATL cases and is known to promote T cell proliferation. In this study, we investigated the hypothesis that HBZ also influences the survival of T cells. Through analyzing the transcriptional profile of HBZ-expressing cells, we learned that HBZ suppressed transcription of the proapoptotic gene *Bim* (*Bcl2l11*) and that HBZ-expressing cells were resistant to activation-induced apoptosis. Mechanistic investigations into how HBZ suppresses *Bim* expression revealed that HBZ perturbs the localization and function of FoxO3a, a critical transcriptional activator of the genes encoding Bim and also Fas ligand (FasL). By interacting with FoxO3a, HBZ not only attenuated DNA binding by FoxO3a but also sequestered the inactive form of FoxO3a in the nucleus. In a similar manner, HBZ also inhibited *FasL* transcription induced by T cell activation. Further study of ATL cells identified other Bim perturbations by HBZ, including at the level of epigenetic alteration, histone modification in the promoter region of the Bim gene. Collectively, our results indicated that HBZ impairs transcription of the *Bim* and *FasL* genes by disrupting FoxO3a function, broadening understanding of how HBZ acts to promote proliferation of HTLV-1-infected T cells by blocking their apoptosis.

Introduction

HTLV-1 is estimated to infect 10-20 million people in the world (1). This virus causes not only a neoplastic disease of $CD4^+$ T cells, ATL, but also chronic inflammatory diseases of the central nervous system, lung, or skin (2). HTLV-1 can be transmitted efficiently in a cell-to-cell fashion (3, 4), while free virus shows poor infectivity (5, 6), and virions are not detected in infected individuals. To increase the number of infected cells and facilitate transmission, HTLV-1 increases its copy number primarily by triggering the proliferation of infected cells -- replicating within the host genome instead of undergoing viral replication (7, 8). Thus, HTLV-1 promotes proliferation and suppresses apoptosis of infected cells via complex interactions of viral proteins with host factors.

Among the viral genes encoded in HTLV-1, the *tax* gene has been extensively studied. Tax can activate various signal pathways like NF-κB, AP-1, and SRF (9). However, Tax expression is frequently undetectable in ATL cases. Importantly, the nonsense mutations in the *tax* gene are often observed in not only ATL cases but also infected cells of asymptomatic HTLV-1 carriers (10). These findings suggest that other mechanisms suppress the apoptosis of HTLV-1 infected cells in the absence of Tax expression (2). We have reported that the *HBZ* gene is expressed in all ATL cases (11). Furthermore, HBZ promotes the proliferation of T-cells and induces development of T-cell lymphomas and inflammatory diseases in transgenic mice (12). Therefore, we speculated that HBZ might also influence apoptosis.

There are two major pathways for apoptosis: the extrinsic and intrinsic apoptotic pathways, which are mediated by Fas and Bim respectively (13). ATL cells are known to express high levels of Fas antigen, and are susceptible to Fas-mediated signaling (14). However, Fas ligand expression is suppressed in ATL cells by silencing of the *early growth response 3 (EGR3)* gene transcription, a phenomenon which enables ATL cells to escape activation-induced cell death (15). In addition, Tax increases expression of c-FLIP, which confers resistance to Fas-mediated apoptosis (16, 17). Furthermore, activation of NF-κB by Tax also enables HTLV-1 infected cells to be resistant to apoptosis (18). To date, the effects of HTLV-1 infection on Bim-mediated apoptosis remain unknown.

In this study, we analyzed transcriptional changes induced by HBZ expression in T cells, and found that transcription of a proapoptotic gene, *Bim*, was hindered by HBZ. This suppression led to decreased activation-induced cell death. We found that HBZ suppressed *Bim* transcription by targeting FoxO3a, a critical transcription factor for the *Bim* and *FasL* gene. In some ATL cell lines and ATL cases, the *Bim* gene transcription was also silenced by epigenetic mechanisms, but this phenomenon appeared to be secondary to HBZ-mediated suppression of transcription. Thus, it is suggested that HBZ suppresses both intrinsic and extrinsic apoptotic pathways and contributes to the proliferation of ATL cells.

Materials and Methods

Cell lines and clinical samples

HTLV-1 immortalized cell lines (MT-4), ATL cell lines **(**ED, TL-Om1, and MT-1), T cell lines not infected with HTLV-1 (Jurkat, SupT1, and CCRF-CEM) were cultured in RPMI 1640 medium supplemented with 10% fetal bovine serum (FBS) and antibiotics at 37°C under a 5% CO_2 atmosphere. Jurkat cells stably expressing spliced form of HBZ (sHBZ), Jurkat-HBZ ,were maintained as described previously (19). To construct CCRF-CEM cells stably expressing HBZ, CEM-HBZ, the coding sequence of HBZ was subcloned into pME18Sneo vector and then the expression vector or its empty vector were transfected into CCRF-CEM cells by using Neon (Invitrogen) according to the manufacturer's instructions. Stable transfectants were selected in G418 (1mg / ml). 293T cells were cultured in Dulbecco modified Eagle medium supplemented with 10% FBS and antibiotics and when 293FT cells were cultured, 500 μg/mL G418 was added. Fas blocking antibody was purchased from Alexis.

This study was conducted according to the principles expressed in the Declaration of Helsinki. The study was approved by the Institutional Review Board of Kyoto University (G204). All patients provided written informed consent for the collection of samples and subsequent analysis.

Plasmid constructs

Wild-type form of FoxO3a was generated by PCR amplification using Jurkat cDNA

library and constitutively active form of FoxO3a (FoxO3aAAA) was also generated by PCR amplification with mutated primers (20). These PCR fragments were then subcloned into pCMV-Tag2B vector and pIRES-hrGFP-1a (Stratagene). The vectors encoding the myc-His-tagged form of HBZ and its mutants used in this study have been described previously (19, 21). We modified pLKO.1-EGFP vector for delivery of anti-FoxO3 short hairpin RNAs to Jurkat, Jurkat-control and Jurkat-HBZ. shRNA sequence used was 5'- GCACAACCTGTCCTGCATAG -3'. The 6xDBE-Luc construct that contains six FOXO-binding sites known as DAF-16 binding elements (DBEs) was kindly provided by Dr. Furuyama (Kagawa Prefectural University of Health Sciences) and the backbone of this vector was pGL3-basic (Promega) (22).

Luciferase assay

Jurkat cells were transfected with 0.2 μg/well of luciferase reporter plasmid, 1 ng/well of *Renilla* luciferase control vector (phRL-TK), 0.2 μg/well of FoxO3aAAA expression plasmid or its empty vector and 0.6 μg/well of HBZ expression plasmid or its empty vector with caspase inhibitor Z-VAD-FMK (MBL). Plasmids were transfected using Neon (Invitrogen) according to the manufacturer's instructions. After 24 hours, cells were collected and luciferase activities were measured using the Dual-Luciferase Reporter Assay (Promega). Relative luciferase activity was calculated as the ratio of firefly to *Renilla* luciferase activity. Three independent experiments, each with triplicate transfections, were performed and typical results are shown.

Microarray analysis

Jurkat-control and Jurkat-HBZ were stimulated with phorbol myristate acetate (PMA) (50 ng/ml) and ionomycin (1 μg/ml) for 9 hrs. After the stimulation, cells were collected and total RNA was isolated using Trizol Reagent (Invitrogen) according to the manufacturer's instructions. We then digested DNA using deoxyribonuclease I (Invitrogen) and cleaned up RNA using RNeasy Mini Kit (Qiagen) according to the manufacturer's instructions. We then synthesized cDNA and performed microarray processing according to the GeneChip Expression Analysis Technical Manual (Affymetrix). All data were analyzed by using GeneSpring GX (Agilent Technologies). The microarray data related to this paper have been submitted to the Gene Expression Omnibus under the accession number GSE48029.

Immunofluorescence analysis

293FT cells were transfected with expression vectors using Lipofectamine LTX (Invitrogen) or TransIT (TAKARA). Twenty-four hours after transfection, cells were re-seeded on the poly-L-lysine coated glass (Matsunami-glass) or poly-D-lysine (SIGMA) coated glass. Twenty-four hours after the re-seeding, cells were fixed with 4% paraformaldehyde for 15 min and permeabilized with 0.2% Triton X-100 for 15min, and blocked by incubation in 5% BSA/PBS for 30 min. For immunostaining, the cells were incubated with anti-Foxo3a, anti-p-Foxo3a (Cell Signaling technology), Cy3-conjugated anti-c-Myc (SIGMA) or biotinylated anti-FLAG (SIGMA) antibodies for 1h or in case of observation of endogenous expression, cells were incubated

overnight at 4°C. Primary antibodies were visualized by incubating the cells with AlexaFluor 488-conjugated goat anti-rabbit IgG antibody (Invitrogen) or Alexa Fluor 488 conjugated streptavidin (Invitrogen). Nuclei were stained and mounted with ProLong Gold antifade reagent with DAPI (Invitrogen). To concentrate non-adherent cells onto a microscope slide, Cytofuge (Statspin) was used. Fixation and blocking were performed as described above.

Assessment of apoptosis

Apoptotic cells were routinely identified by Annexin V-APC (eBioscience) or PE or FITC (BioVision) staining according to the manufacturer's instructions and analyzed with a flow cytometer (BD FACSCanto II, BD Biosciences). Data files were analyzed by using FlowJo software (Treestar).

Real-time PCR

Total RNA was isolated for the analysis using Trizol reagent. RNA was treated with DNase I to eliminate the genomic DNA. Reverse transcription was performed using random primer and SuperScript III reverse transcriptase (Invitrogen). CD25-CD4+ cells from healthy donor were obtained by using human CD4 T Lymphocyte enrichment kit (BD Pharmingen). Then cells were stimulated with PMA/Io for 9 hrs and RNA was isolated and reverse transcription were performed as described above. cDNA products were analyzed by real-time PCR using the Taqman Universal PCR Master Mix (PE Applied Biosystems) or Fast Start Universal SYBR Green master (Roche) and Applied

Biosystems StepOnePlus real-time PCR system according to the manufacturer's instructions. Specific primers and Taqman probes for the *Bim* gene, *FasL* gene and *GAPDH* internal control gene were purchased from Applied Biosystems. Primer sequences for the *HBZ* gene and *GAPDH* gene used for the evaluation of the knock down efficiency in MT-1 cells are described previously (11, 23). Primer sequences for the *HBZ* gene used for another experiment to evaluate the HBZ expression in Jurkat-HBZ, MT-1, TL-Om1, and ED cells were 5'-ATGGCGGCCTCAGGGCTGTT-3' and 5'- GCGGCTTTCCTCTTCTAAGG-3**'.** Primer sequences for the *FoxO3a* gene used were 5'-ACAAACGGCTCACTCTGTCCCAG -3' and 5'-AGCTCTTGCCAGTTCCCTCATTCTG -3'. All amplifications were conducted in triplicates. The relative quantification was calculated according to the method described in Applied Biosystems ABI prism 7700 SDS User Bulletin #2.

Chromatin immunoprecipitation (ChIP) analysis

Chromatin immunoprecipitation (ChIP) assay was performed according to the protocol recommended by Millipore. Cells were fixed with 1% formaldehyde for 10 minutes at room temperature, washed twice with ice-cold PBS, treated with SDS-lysis buffer [1% SDS, 50 mM EDTA and 200 mM Tris-HCl] for 10 minutes on ice and then sonicated. Thereafter, the DNA/protein complexes were immunoprecipitated with antibodies specific for acetylated-Histone H3, acetylated-Histone H4, dimethylated-Histone H3 (Lys4), RNA polymerase II clone CTD4H8 (Millipore),

trimethylated-Histone H3 (Lys27), anti-trimethyl-Histone H3 (Lys9) antibodies (Cell Signaling technology), or normal rabbit IgG (Santa Cruz technology) overnight at 4°C . Immune complexes were collected with salmon sperm DNA-protein A and G Sepharose slurry, washed, and eluted with freshly prepared elution buffer (1% SDS, 100 mM NaHCO3). Protein-DNA complexes were de-crosslinked at 65°C for 4 hours. DNA was purified and subjected to real-time PCR for quantification of the target fragments. Sequences for the primer set are described previously (24, 25). For the evaluation of binding of FoxO3a to the FOXO-binding sites, 293T cells were transfected with the 5 μg of 6xDBE-Luc construct, 5 μg of FoxO3aAAA expression plasmid together with or without 5 μg of HBZ plasmid using TransIT in 10-cm dishes. Anti-Flag (SIGMA) antibody was used for the immunoprecipitation. Primers used were 5'-AGTGCAGGTGCCAGAACATT-3' and 5'-GCCTTATGCAGTTGCTCTCC-3' which were constructed inside of the pGL3-basic vector. For the evaluation of the DNA binding capacity of FoxO3a with or without HBZ, expression vectors for the HA-tagged FoxO3a and Flag-tagged HBZ were transiently cotransfected into 293T cells using the TransIT reagent. 24 hours after the transfection, cells were collected and chromatin immunoprecipitation assay was performed as described above. For the immunoprecipitation, anti-HA (SIGMA) antibody was used. Primers used for *Bim* gene promoter were 5'- CCACCACTTGATTCTTGCAG-3' and 5'-TCCAGCGCTAGTCTTCCTTC-3' which were constructed to contain the FOXO-binding sequence located in intron1. Primers used for *FasL* gene promoter were 5'- ACGATAGCACCACTGCACTCC -3' and 5'- GGCTGCAAACCAGTGGAAC

-3’which were also constructed to contain the three FOXO-binding sequences.

Individual PCRs were carried out in triplicate to control for PCR variation and mean C_t values were collected. Fold difference of the antibody-bound fraction (*IP*) versus a fixed amount of input (*In*) was calculated as

$$IP/In = 2^{-\Delta\Delta C_t} = 2^{-(C_t\,(IP)-C_t(In))}$$

Then, the fold difference value for a target antibody (*t*) was subtracted by the nonspecific value derived from mouse or rabbit IgG (t_0) ;

$$(IP/In)^t - (IP/In)^{t_0} \quad .$$

Bisulfite genomic sequencing

Sodium bisulfite treatment of genomic DNA was performed as described previously (26). DNA regions were amplified using bisulfite-treated genomic DNA by nested PCR. To amplify promoter region (promoter 1) of *Bim*, primers used in the first PCR were 5’-TTTAGAGGGAGGAGAGTTTAAAG-3’ and 5’-CCCTACAACCCAACTCTAACTA-3’. Primers for the second PCR were 5’-AGGGTATAGTGAGAGCGTAGG-3’ and 5’-CAACTCTAACTAACGACCCC-3’. For promoter 2 primers used in the first PCR were 5’-GTGTGATTGTTTTTTGAGGG-3’ and 5’- AAAATACCCCCAAACAAAATAC-3’. Primers for the second PCR were 5’- GCGGATTTAGTTGTAGATTTTG-3’ and 5’-ACTCTTTACCCAAAACAAACTTC-3’. PCR products were purified, cloned into pGEM-T Easy vector (Promega), and sequenced using the ABI PRISM 3130 genetic analyzer. For CpG methylation analysis, web-based bisulfite sequencing analysis tool

called QUMA (quantification tool for methylation analysis) was used (27).

Coimmunoprecipitation assay, analysis of the p-FoxO3a localization and immunoblotting

Expression vectors for the relevant genes were transiently cotransfected into 293T cells using the TransIT reagent. 48 hours later, cells were collected and coimmunoprecipitation assays were performed as described previously (28). For the analysis of the p-FoxO3a localization, nuclear and cytoplasmic proteins were extracted using Nuclear Complex Co-IP Kit (Active motif). The proteins were subjected to SDS-PAGE analysis followed by immunoblotting with various antibodies. Antibodies used were anti-p-FoxO3a, anti-α-tublin (SIGMA), anti-Flag, anti-HA (SIGMA), and anti- His (MBL).

Lentiviral vector construction and transfection of the recombinant lentivirus

Lentiviral vector expressing shRNA against HBZ was constructed and recombinant lentivirus was infected as described previously (11). When > 90% of cells expressed EGFP, the *HBZ* and *Bim* genes expressions were analyzed by real-time PCR.

Results

The *Bim* gene transcription is suppressed in HBZ-expressing Jurkat and CCRF-CEM cells

To determine the effects of HBZ on gene expression, we first performed microarray analysis. Jurkat cells with or without expression of spliced form of HBZ (Jurkat-HBZ and Jurkat-control, respectively) were stimulated with PMA and ionomycin (Io) for 9 hrs. Gene expression profiles were then analyzed by DNA microarray. Table 1 shows the apoptosis-associated genes that were down-regulated or up-regulated in stimulated Jurkat-HBZ cells. Transcription of the *Bim* gene was prominently down-regulated in HBZ-expressing Jurkat cells. To confirm the effect of HBZ on the *Bim* gene expression, we evaluated *Bim* mRNA levels in Jurkat-control and Jurkat-HBZ cells with or without PMA/Io stimulation using real-time PCR. As reported in the previous studies showing that treatment by PMA/Io or other stimulators induced *Bim* expression (29, 30), the *Bim* mRNA level of stimulated Jurkat-control cells was three-times higher than that of unstimulated cells, but that of Jurkat-HBZ cells did not change after stimulation (Figure 1A). Similarly, increased *Bim* transcription by stimulation was also inhibited by HBZ in CCRF-CEM cells (Figure 1A).

HBZ inhibits apoptosis

It has been reported that Bim plays an important role in activation induced cell death and T cell homeostasis (31). Since the above data demonstrated that HBZ inhibits

stimulation-induced *Bim* expression, we next investigated whether HBZ inhibits apoptosis in response to PMA/Io stimulation. To test this, Jurkat-control and Jurkat-HBZ were each incubated with or without PMA/Io for 9 hours, and then apoptosis was measured using Annexin V. The percentages of apoptotic cells in Jurkat-control and Jurkat-HBZ were 40.2 % and 15 % respectively, indicating that HBZ suppressed activation-induced apoptosis (Figure 1B). We also treated cells with doxorubicin and found that HBZ slightly inhibited doxorubicin-induced apoptosis (Supplementary Fig. S1). Fas-mediated apoptotic pathway might be involved in anti-apoptotic effect by HBZ. In order to assess the effect of Fas-mediated signaling on the activation-induced apoptosis, cells were also treated with or without Fas blocking antibody (0.5 μg/ml) 30 min before the PMA/Io stimulation. The percentage of apoptotic cells without Fas blocking antibody in Jurkat-control and Jurkat-HBZ were 36.9 % and 22.4 %, respectively. When cells were treated with Fas blocking antibody, the percentage of apoptotic cells reduced and those were 24 % and 13.2 % in Jurkat-control and Jurkat-HBZ, respectively (Figure 1C). Thus, Fas blocking antibody partially inhibited apoptosis in Jurkat-HBZ, which indicates that Fas-mediated signals are also implicated in activation-induced cell death. Indeed, we found that the transcription level of *FasL* was suppressed in stimulated Jurkat-HBZ and CEM-HBZ cells compared with Jurkat-control and CEM-control cells (Figure 1D), suggesting that down-regulation of FasL by HBZ was also associated with inhibition of apoptosis.

HBZ suppresses *Bim* expression through attenuation of FoxO3a

We analyzed how HBZ suppresses the expression of *Bim* and *FasL*. It has been reported that a Forkhead factor, FoxO3a, and p73 are important for the transcription of *Bim* and *FasL* (32, 33). FoxO3a and other FOXO family members are phosphorylated by protein kinases such as Akt or SGK on highly conserved serine and threonine residues (especially Thr32, Ser253, Ser315 in FoxO3a), resulting in impaired DNA binding activity and increased binding to the chaperone protein, 14-3-3 (20, 34, 35). Newly formed 14-3-3-FOXO complexes are then exported from the nucleus, thereby inhibiting FOXO-dependent transcription of key target genes such as *Bim*, *FasL* and *TRAIL* (36).

First, we investigated whether FoxO3a is implicated for the activation induced cell death. As shown in supplementary Fig. S2, the knockdown of FoxO3a resulted in the decreased apoptotic rate in Jurkat-control cells ($p < 0.05$). Furthermore, inhibition of Foxo3a did not influence activation-induced cell death in Jurkat-HBZ cells, suggesting that inhibitory effect of HBZ on Foxo3a function. To investigate whether HBZ affects FoxO3a function, Jurkat cells were transiently transfected with a plasmid expressing FoxO3aAAA, the constitutive active mutant of FoxO3a, which is no longer phosphorylated by Akt and is localized in the nucleus. The FoxO3aAAA was expressed together with hrGFP using an internal ribosome entry site (IRES) (FoxO3aAAA-IREShrGFP). Jurkat cells were transiently transfected with full-length HBZ or its mutants. HBZ has 3 domains, an activation domain (AD), a central domain (CD), and a basic leucine zipper domain (bZIP) (12). In this study the deletion mutants (HBZ-ΔAD, HBZ- ΔbZIP, and HBZ-ΔCD) were used. The percentage of FoxO3aAAA

induced apoptotic cells in the absence of HBZ was 69.6 % while it was suppressed by HBZ (40.6 %, $p < 0.001$) (Figure 2A). We also found that an HBZ mutant without activation domain lacks the activity to inhibit FoxO3aAAA-induced apoptosis (Figure 2A), indicating the significance of activation domain in suppression of FoxO3a mediated apoptosis. It has been reported that LXXLL motif in FoxO3a binds to its coactivator CBP/p300 (37). Similarly, HBZ has LXXLL-like motifs located in the NH_2-terminal region, which bind to KIX domain of CBP/p300 (38). We speculated that the LXXLL-like motifs of HBZ might affect FoxO3aAAA function through KIX domain of CBP/p300. An HBZ mutant, which has substitutions in 27th and 28th residues (LL to AA) of LXXLL-like motif, lack the activity to suppress FoxO3aAAA mediated apoptosis (Figure 2B), indicating that LXXLL-like motif of HBZ is critical for suppression of FoxO3a mediated apoptosis.

Next, we analyzed the effect of HBZ on a FoxO3a responsive reporter. As shown in Figure 2C, HBZ suppressed FoxO3a mediated transcriptional activity ($p < 0.01$). In order to check whether HBZ inhibits DNA binding of FoxO3a, 293T cells were transiently transfected with FoxO3aAAA and FoxO3a reporter, 6xDBE-Luc, together with or without HBZ. The interaction of FoxO3aAAA to FOXO-binding sites was analyzed by ChIP assay. As shown in Figure 2D, the interaction of FoxO3aAAA to the FOXO-binding sites was interfered by HBZ, suggesting that HBZ inhibits FoxO3a-mediated apoptosis through suppression of the DNA binding of FoxO3a. In order to clarify the mechanism of HBZ-mediated FoxO3a inhibition, we examined interaction between HBZ and FoxO3a by the immunoprecipitation assay. It showed that

HBZ interacted with FoxO3a (Figure 2E, F). Experiments with FoxO3a deletion mutant revealed that HBZ interacted with the forkhead domain (FH) of FoxO3a (Figure 2E). Analysis using HBZ deletion mutants showed that the central domain of HBZ interacted with FoxO3a (Figure 2F).

HBZ inhibits nuclear export of phosphorylated form of FoxO3a

Next we investigated the effect of HBZ on FoxO3a localization by confocal microscopy. We co-transfected 293FT cells with a plasmid expressing human wild-type FoxO3a (FoxO3aWT) protein and an HBZ-expressing plasmid. Consistent with previous reports, FoxO3a remained mainly in cytoplasm when cells were co-transfected with empty vector (Figure 3A) (20, 34). However, when it was expressed along with HBZ, FoxO3a was localized in both nucleus and cytoplasm (Figure 3A). To determine whether mislocalized FoxO3a is phosphorylated (pFoxO3a) or not, we used anti-pFoxO3a antibody. Figure 3B and 3C demonstrated that nuclear-localized FoxO3a was phosphorylated in HBZ expressing cells. Thereafter, we analyzed the localization of endogenous FoxO3a in HeLa and an ATL cell line, MT-1. Although pFoxO3a was localized widely both in cytoplasm and nucleus in HeLa cells, most pFoxO3a was localized in the nucleus in MT-1 (Figure 3D), suggesting that endogenous HBZ inhibits the extranuclear translocation of pFoxO3a in this cell line. From the study of crystal structure of the human FoxO3a-DBD/DNA complex, it has been reported that phosphorylation at Ser253 causes a decrease on the DNA binding ability (39). Abnormal localization of phosphorylated FoxO3a by HBZ might interfere the function

of unphosphorylated FoxO3a in the nucleus. The abnormal localization of pFoxO3a prompted us to investigate whether HBZ bound to 14-3-3 along with FoxO3a, since 14-3-3 is a chaperon protein involved in nuclear-cytoplasm shuttling of FOXO family. As shown in Figure 3E, HBZ, FoxO3a and 14-3-3 form a ternary complex. However, the binding of FoxO3a and 14-3-3 was not affected by HBZ (result of IP with anti-Flag Ab and detected with anti-HA Ab).

As another possible mechanism for down-regulation of *Bim* and *FasL*, we compared the transcription level of *p73* in Jurkat cells with and without HBZ expression. Activation of HBZ expressing cells reduced transcription of *p73*, but the expression level of *p73* was variable among ATL cell lines (Supplementary Fig. S3A, B). We conclude that p73 is not responsible for suppression of *Bim* expression in ATL cells.

Bim expression is suppressed in both ATL cell lines and ATL cases

HBZ has been shown to suppress Bim expression through two different mechanisms as revealed in this study. To analyze Bim expression in ATL cells, we studied *Bim* mRNA levels in non-ATL cell lines and ATL cell lines with or without PMA/Io stimulation, and found that the *Bim* gene transcript was up-regulated in Jurkat and CCRF-CEM cells, but not in SupT1 after activation. However, *Bim* transcripts were not increased in all stimulated ATL cell lines (Figure 4A). The *Bim* gene transcript was also down-regulated in primary ATL cells (Figure 4B) compared with resting PBMCs and PHA stimulated T cells. We also stimulated primary ATL cells and normal CD4+ T cells with PMA/Io. The *Bim* gene transcription was quite low in primary ATL sample

compared with normal CD4+ T cells even though cells were stimulated with PMA/Io (Figure 4C). In order to confirm HBZ expression in representative ATL cell lines, we quantified the level of the *HBZ* mRNA transcription in Jurkat-HBZ, CEM-HBZ, MT-1, ED and TL-Om1 by real-time PCR and confirmed that HBZ is expressed in these ATL cell lines (Supplementary Fig. S4). A microarray data obtained from Gene Expression Omnibus (GEO), shows that both *Bim* and *FasL* transcription levels are lower in ATL cases than healthy donors (accession number: GSE33615, Supplementary Fig. S5), supporting our data that *Bim* expression was suppressed in ATL cells.

Bim **expression is silenced by epigenetic mechanisms**

Since the *Bim* gene transcription was severely suppressed in ATL cells, we investigated the epigenetic status (DNA methylation and histone modification) of the promoter region of the *Bim* gene in ATL cells. A previous study showed that the 0.8 kb region immediately upstream of exon 1 contains the important elements for the control of *Bim* expression (promoter 1). The *Bim* promoter does not contain a TATA or CAAT box and has the characteristics of a 'TATA-less' promoter (40). Additionally, the alternative promoter has been reported to exist in intron 1 (promoter 2) (41, 42). These two promoter regions are highly GC-rich and contain the binding sites for several transcription factors including FoxO3a. To determine whether CpG sites in these *Bim* gene promoter regions are methylated in ATL cell lines, their methylation status was analyzed by bisulfite-mediated methylcytosine mapping (Supplementary Fig. S6A, B). The promoter 1 of *Bim* was hypermethylated in two ATL cell lines (ED and TL-Om1),

and ATL case 1 while this region was not so methylated in MT-1 cells and two ATL cases. On the other hand, the promoter 2 was heavily methylated in two ATL cell lines (TL-Om1 and MT-1) and ATL case 1 and partially methylated in Jurkat cells (Supplementary Fig. S6B). These results suggest that in some cases, heavily methylated CpG sites of promoter 1 and 2 are associated with silencing of *Bim* transcription but these methylations can not account for suppressed *Bim* expression in all ATL cell lines and ATL cases.

Therefore, we next focused on the histone modification in the promoter region of *Bim*. It is well known that deacetylation of the histones are also common features of cancer, which results in transcriptional silencing of tumor suppressor genes (43). First, we analyzed the histone H3 and H4 acetylation and H3K4 trimethylation, which are all permissive marks (44), in promoter 1 of Jurkat, MT-1, and TL-Om1 cells. Contrary to our speculation, neither H3, H4 acetylation nor H3K4 trimethylation did not differ between MT-1 and Jurkat cells (Supplementary Fig. S7). We next analyzed the histone modification status in promoter 2. As shown in Figure 5A, MT-1 and TL-Om1 cells exhibited decreased level of histone H3 acetylation and H3K4 trimethylation but not histone H4 acetylation. Since methylation of DNA is often preceded by dimethylation of H3K9 or trimethylation of H3K27 (both repressive marks) in oncogenesis (44), we asked whether there were differences in these epigenetic chromatin marks on the *Bim* gene promoter in ATL cell lines. TL-Om1 cells exhibited upregulated level of H3K9 dimethylation and H3K27 trimethylation compared to Jurkat cells (Figure 5B, C) while MT-1 exhibited a little upregulated level of H3K27 trimethylation (Figure 5C) in the

promoter 2. These data suggest that histone modifications of promoter 2 are critical for the suppressed *Bim* gene transcription. We also performed ChIP analysis using anti-RNA polymerase II antibody (Figure 5D) and revealed that Pol II binding was decreased in MT-1 and TL-Om1 cells, confirming suppressed transcription of the *Bim* gene. To further investigate the mechanisms involved in FoxO3a-mediated *Bim* gene transcription in the promoter 2, we transfected HA-tagged FoxO3a expression vector together with or without a HBZ expression vector into 293T cells and immunoprecipitated with anti-HA antibody. Then the DNA binding capacity of FoxO3a was quantified by real-time PCR. Figure 5E shows that HBZ attenuated the DNA binding capacity of FoxO3a in the promoter 2 of *Bim* (i) and *FasL* promoter (ii), suggesting that the suppressed binding of FoxO3a to the promoter regions leads to inhibition of the *Bim* and *FasL* genes transcription by HBZ.

Next we treated MT-1 cells with trichostatin A (TSA), a cell-permeable chemical inhibitor of class I/II HDACs. Treatment of TSA resulted in a clear up-regulation of acetylation of histone H3 (Figure 5F) followed by Bim expression both at the mRNA (Figure 5G) and protein levels (Figure 5H), indicating that histone modification is associated with suppressed *Bim* transcription in MT-1. We also performed ChIP assay using Jurkat-control and Jurkat-HBZ cells, which were stimulated with PMA and ionomycin for 9h, and found that acetylation of histone H3 decreased in Jurkat-HBZ cells (Figure 5I), suggesting that HBZ is implicated in histone deacetylation in T-cells. To verify whether HBZ inhibits transcription of the *Bim* gene, we suppressed the *HBZ* gene transcription by shRNA as reported previously (11). Efficiencies of lentivirus

vector transduction, which were determined by EGFP expression, were 90.5 % and 90.3 % for control MT-1 cells and HBZ-knockdown MT-1 cells, respectively. Suppressed HBZ expression led to increased the *Bim* gene transcription (Figure 5J, K), indicating that HBZ expression is linked to suppression of *Bim* expression in ATL cells.

Discussion

Human immunodeficiency virus type 1 (HIV-1) replicates vigorously, and the generated virus infects target cells *in vivo*. Unlike HIV-1, HTLV-1 induces proliferation to increase the number of infected cells, since this virus is transmitted primarily by cell-to-cell contact (5). Therefore, HTLV-1-encoded proteins promote proliferation of infected cells and inhibit their apoptosis, resulting in an increased number of infected cells *in vivo* (2). In this study, we show that HBZ inhibits both the intrinsic and extrinsic apoptotic pathways via targeting FoxO3a, which leads to suppressed transcriptions of *Bim* and *FasL*. We demonstrated two mechanisms for perturbation of FoxO3a by HBZ; interaction of HBZ with FoxO3a and interference of nuclear export of phosphorylated FoxO3a. HBZ suppresses DNA binding ability of active form of FoxO3a through interaction between central domain of HBZ and FH domain of FoxO3a. In addition, LXXLL-like motif of HBZ is implicated in inhibition of FoxO3a mediated apoptosis, suggesting that HBZ interferes interaction of CBP/p300 and FoxO3a. Furthermore, HBZ retains inactive form of FoxO3a in the nucleus through interaction with 14-3-3, leading to transcriptional repression of the target genes. Interestingly, accumulation of phosphorylated form of FoxO3a in the nucleus has been observed in HIV Vpr-expressing cells, which might be implicated in HIV-mediated resistance against insulin (28). Thus, FoxO3a is a target of both human retroviruses.

In this study, we showed that central domain of HBZ interacts with FoxO3a while LXXLL-like motif in activation domain of HBZ is responsible for suppressed apoptosis.

LXXLL-like motif of HBZ has been reported to interact with KIX domain of p300 (38). The central domain of HBZ interacts with the FH domain of FoxO3a, which binds to the target sequence (35). This is mechanism how HBZ inhibits DNA binding of FoxO3a. However, inhibitory effect of HBZ on apoptosis largely depends on LXXLL-like motif of activation domain (Figure 2A and B). FoxO3a is also reported to interact with KIX domain of CBP/p300 (37). FH domain of FoxO3a intramolecularly interacts with its conserved regions (CR) 3, and binding of FH to DNA releases CR3, allowing it to bind KIX of CBP/p300 (45). These findings suggest that HBZ interferes the complex interaction between FoxO3a and CBP/p300, which is likely important to induce apoptosis.

It has been reported that Bim has a tumor suppressor function in various cancers. Hemizygous loss of the *Bim* gene promoted development of B-cell leukemia in Myc-transgenic mice in which c-myc expression was driven by the immunoglobulin gene intron-enhancer (46). Insulin-like growth factor 1 (IGF-1), an important growth factor for myeloma cells, has been reported to suppress Bim expression by epigenetic and posttranslational mechanisms (25). In Epstein-Barr virus infected B cells *Bim* transcription is silenced by DNA methylation of the *Bim* gene promoter (47). Thus, impaired expression of Bim is associated with the various cancers including the virus-related malignancies. FoxO3a is also a target of oncogenesis. BCR-ABL induces phosphorylation of FoxO3a, which leads to suppressed expression of Bim in Ph1+ chronic myelogenous leukemia cells (32). In breast cancer, IκB kinase interacts with, phosphorylates FoxO3a, which causes proteolysis of FoxO3a (48). In this study, we

revealed that HBZ hinders nuclear export of phosphorylated FoxO3a, and impairs function of FoxO3a likely through interaction of FoxO3a and p300. Thus, suppressed Bim and FasL expression through inhibition of FoxO3a by HBZ is a new mechanism for oncogenesis.

Besides of FoxO3a perturbation by HBZ, we also have identified the epigenetic aberrations in the promoter region of the *Bim* gene in ATL cells, and found that Bim expression is suppressed by DNA methylation and histone modification. ATL cell lines exhibited upregulated level of H3K27 trimethylation in the promoter regions of *Bim*. It has been reported that enhancer of zeste (EZH) 2, a methyltransferase and component of the polycomb repressive complex 2 (PRC2), expression is increased in ATL cell lines (42). Since EZH2 plays an essential role in the epigenetic maintenance of H3K27 trimethylation, upregulated H3K27 trimethylation of the *Bim* gene promoter might be associated with increased expression of EZH2 in ATL cells. In addition, HBZ seems to be associated with histone deacetylation in MT-1 cells. According to the previous studies, it is known that both HBZ and FoxO3a bind to the histone acetyltransferase p300/CBP through the LXXLL motif (38). In this study, we found that the same motif is important for FoxO3a suppression and resulting inhibition of apoptosis. It is likely that HBZ decreases histone acetylation level on Bim promoter through the interaction with FoxO3a and dissociation of p300/CBP from the promoter. In addition to histone modifications, hypermethylation of CpGs in Bim promoter was observed in some ATL cells. These epigenetic aberrations likely occur as the secondary changes following long time silencing of *Bim* by HBZ, although the further investigations will be required.

In this study, we demonstrated that HBZ suppresses activation-induced apoptosis by down-regulation of pro-apoptotic genes, *Bim* and *FasL*. HBZ perturbs the function of FoxO3a by interaction, and induces epigenetic aberrations in the promoter region of the *Bim* gene. It has been shown that HBZ induces not only cancer but also inflammation *in vivo*. Since inflammatory diseases are essentially caused by failure to negatively regulate unnecessary immune responses by apoptosis, suppression of apoptosis by HBZ might be associated with HTLV-1-induced inflammation as well. Collectively, HBZ-mediated inhibition of apoptosis is likely implicated in both neoplastic and inflammatory diseases caused by HTLV-1.

Author Contributions

Conception and design: A. T. Nakanishi, K. Takai, J. Yasunaga, M. Matsuoka

Development of methodology: A. T. Nakanishi, K. Takai, J. Yasunaga, M. Matsuoka

Acquisition of data (provided animals, acquired and managed patients, provided facilities, etc.): A. T. Nakanishi, K. Takai

Analysis and interpretation of data (e.g., statistical analysis, biostatistics, computational analysis): A. T. Nakanishi, K. Takai, J. Yasunaga, M. Matsuoka

Writing, review, and/or revision of the manuscript: A. T. Nakanishi, J. Yasunaga, M. Matsuoka

Administrative, technical, or material support (i.e., reporting or organizing data, constructing databases): A. T. Nakanishi, K. Takai, J. Yasunaga, M. Matsuoka

Study supervision: M. Matsuoka

Acknowledgements

We thank T. Furuyama (Kagawa Prefectural University of Health Science) for the 6xDBE-Luc plasmid DNA, P. Bouillet for valuable comments on this study, and L. Kingsbury for proofreading of this manuscript.

Grant Support: This study was supported by a Grant-in-aid for Scientific Research from the Ministry of Education, Science, Sports, and Culture of Japan, to M. M. (MEXT grant number 221S0001) a grant from Japan Leukemia Research Fund to M.M. and a grant from the Takeda Science Foundation to J.Y.

References

1. Proietti FA, Carneiro-Proietti AB, Catalan-Soares BC, Murphy EL. Global epidemiology of HTLV-I infection and associated diseases. Oncogene. 2005;24:6058-68.

2. Matsuoka M, Jeang KT. Human T-cell leukaemia virus type 1 (HTLV-1) infectivity and cellular transformation. Nat Rev Cancer. 2007;7:270-80.

3. Igakura T, Stinchcombe JC, Goon PK, Taylor GP, Weber JN, Griffiths GM, et al. Spread of HTLV-I between lymphocytes by virus-induced polarization of the cytoskeleton. Science. 2003;299:1713-6.

4. Pais-Correia AM, Sachse M, Guadagnini S, Robbiati V, Lasserre R, Gessain A, et al. Biofilm-like extracellular viral assemblies mediate HTLV-1 cell-to-cell transmission at virological synapses. Nat Med. 2010;16:83-9.

5. Derse D, Hill SA, Lloyd PA, Chung H, Morse BA. Examining human T-lymphotropic virus type 1 infection and replication by cell-free infection with recombinant virus vectors. J Virol. 2001;75:8461-8.

6. Mazurov D, Ilinskaya A, Heidecker G, Lloyd P, Derse D. Quantitative comparison of HTLV-1 and HIV-1 cell-to-cell infection with new replication dependent vectors. PLoS pathogens. 2010;6:e1000788.

7. Cavrois M, Leclercq I, Gout O, Gessain A, Wain-Hobson S, Wattel E. Persistent oligoclonal expansion of human T-cell leukemia virus type 1-infected circulating cells in patients with Tropical spastic paraparesis/HTLV-1 associated

myelopathy. Oncogene. 1998;17:77-82.

8. Etoh K, Tamiya S, Yamaguchi K, Okayama A, Tsubouchi H, Ideta T, et al. Persistent clonal proliferation of human T-lymphotropic virus type I-infected cells in vivo. Cancer Res. 1997;57:4862-7.

9. Grassmann R, Aboud M, Jeang KT. Molecular mechanisms of cellular transformation by HTLV-1 Tax. Oncogene. 2005;24:5976-85.

10. Fan J, Ma G, Nosaka K, Tanabe J, Satou Y, Koito A, et al. APOBEC3G Generates Nonsense Mutations in HTLV-1 Proviral Genomes In Vivo. J Virol. 2010.

11. Satou Y, Yasunaga J, Yoshida M, Matsuoka M. HTLV-I basic leucine zipper factor gene mRNA supports proliferation of adult T cell leukemia cells. Proc Natl Acad Sci U S A. 2006;103:720-5.

12. Satou Y, Yasunaga J, Zhao T, Yoshida M, Miyazato P, Takai K, et al. HTLV-1 bZIP Factor Induces T-Cell Lymphoma and Systemic Inflammation In Vivo. PLoS pathogens. 2011;7:e1001274.

13. Bouillet P, O'Reilly LA. CD95, BIM and T cell homeostasis. Nat Rev Immunol. 2009;9:514-9.

14. Debatin KM, Goldman CK, Waldmann TA, Krammer PH. APO-1-induced apoptosis of leukemia cells from patients with adult T-cell leukemia. Blood. 1993;81:2972-7.

15. Yasunaga J, Taniguchi Y, Nosaka K, Yoshida M, Satou Y, Sakai T, et al. Identification of aberrantly methylated genes in association with adult T-cell leukemia. Cancer Res. 2004;64:6002-9.

16. Krueger A, Fas SC, Giaisi M, Bleumink M, Merling A, Stumpf C, et al. HTLV-1 Tax protects against CD95-mediated apoptosis by induction of the cellular FLICE-inhibitory protein (c-FLIP). Blood. 2006;107:3933-9.

17. Okamoto K, Fujisawa J, Reth M, Yonehara S. Human T-cell leukemia virus type-I oncoprotein Tax inhibits Fas-mediated apoptosis by inducing cellular FLIP through activation of NF-kappaB. Genes to cells : devoted to molecular & cellular mechanisms. 2006;11:177-91.

18. Sun SC, Yamaoka S. Activation of NF-kappaB by HTLV-I and implications for cell transformation. Oncogene. 2005;24:5952-64.

19. Zhao T, Yasunaga J, Satou Y, Nakao M, Takahashi M, Fujii M, et al. Human T-cell leukemia virus type 1 bZIP factor selectively suppresses the classical pathway of NF-kappaB. Blood. 2009;113:2755-64.

20. Brunet A, Bonni A, Zigmond MJ, Lin MZ, Juo P, Hu LS, et al. Akt promotes cell survival by phosphorylating and inhibiting a Forkhead transcription factor. Cell. 1999;96:857-68.

21. Zhao T, Satou Y, Sugata K, Miyazato P, Green PL, Imamura T, et al. HTLV-1 bZIP factor enhances TGF-{beta} signaling through p300 coactivator. Blood. 2011;118:1865-76.

22. Furuyama T, Nakazawa T, Nakano I, Mori N. Identification of the differential distribution patterns of mRNAs and consensus binding sequences for mouse DAF-16 homologues. The Biochemical journal. 2000;349:629-34.

23. Ponchel F, Toomes C, Bransfield K, Leong FT, Douglas SH, Field SL, et al.

Real-time PCR based on SYBR-Green I fluorescence: an alternative to the TaqMan assay for a relative quantification of gene rearrangements, gene amplifications and micro gene deletions. BMC Biotechnol. 2003;3:18.

24. Richter-Larrea JA, Robles EF, Fresquet V, Beltran E, Rullan AJ, Agirre X, et al. Reversion of epigenetically mediated BIM silencing overcomes chemoresistance in Burkitt lymphoma. Blood. 2010;116:2531-42.

25. De Bruyne E, Bos TJ, Schuit F, Van Valckenborgh E, Menu E, Thorrez L, et al. IGF-1 suppresses Bim expression in multiple myeloma via epigenetic and posttranslational mechanisms. Blood. 2010;115:2430-40.

26. Fan J, Kodama E, Koh Y, Nakao M, Matsuoka M. Halogenated thymidine analogues restore the expression of silenced genes without demethylation. Cancer Res. 2005;65:6927-33.

27. Kumaki Y, Oda M, Okano M. QUMA: quantification tool for methylation analysis. Nucleic Acids Res. 2008;36:W170-5.

28. Kino T, De Martino MU, Charmandari E, Ichijo T, Outas T, Chrousos GP. HIV-1 accessory protein Vpr inhibits the effect of insulin on the Foxo subfamily of forkhead transcription factors by interfering with their binding to 14-3-3 proteins: potential clinical implications regarding the insulin resistance of HIV-1-infected patients. Diabetes. 2005;54:23-31.

29. Cante-Barrett K, Gallo EM, Winslow MM, Crabtree GR. Thymocyte negative selection is mediated by protein kinase C- and Ca2+-dependent transcriptional induction of bim [corrected]. Journal of immunology. 2006;176:2299-306.

30. Snow AL, Oliveira JB, Zheng L, Dale JK, Fleisher TA, Lenardo MJ. Critical role for BIM in T cell receptor restimulation-induced death. Biol Direct. 2008;3:34.

31. Green DR, Droin N, Pinkoski M. Activation-induced cell death in T cells. Immunological reviews. 2003;193:70-81.

32. Essafi A, Fernandez de Mattos S, Hassen YA, Soeiro I, Mufti GJ, Thomas NS, et al. Direct transcriptional regulation of Bim by FoxO3a mediates STI571-induced apoptosis in Bcr-Abl-expressing cells. Oncogene. 2005;24:2317-29.

33. Busuttil V, Droin N, McCormick L, Bernassola F, Candi E, Melino G, et al. NF-kappaB inhibits T-cell activation-induced, p73-dependent cell death by induction of MDM2. Proc Natl Acad Sci U S A. 2010;107:18061-6.

34. Brunet A, Park J, Tran H, Hu LS, Hemmings BA, Greenberg ME. Protein kinase SGK mediates survival signals by phosphorylating the forkhead transcription factor FKHRL1 (FOXO3a). Molecular and cellular biology. 2001;21:952-65.

35. Obsil T, Obsilova V. Structure/function relationships underlying regulation of FOXO transcription factors. Oncogene. 2008;27:2263-75.

36. Modur V, Nagarajan R, Evers BM, Milbrandt J. FOXO proteins regulate tumor necrosis factor-related apoptosis inducing ligand expression. Implications for PTEN mutation in prostate cancer. J Biol Chem. 2002;277:47928-37.

37. Wang F, Marshall CB, Yamamoto K, Li GY, Gasmi-Seabrook GM, Okada H, et al. Structures of KIX domain of CBP in complex with two FOXO3a transactivation domains reveal promiscuity and plasticity in coactivator recruitment. Proc Natl Acad Sci U S A. 2012;109:6078-83.

38. Clerc I, Polakowski N, Andre-Arpin C, Cook P, Barbeau B, Mesnard JM, et al. An interaction between the human T cell leukemia virus type 1 basic leucine zipper factor (HBZ) and the KIX domain of p300/CBP contributes to the down-regulation of tax-dependent viral transcription by HBZ. J Biol Chem. 2008;283:23903-13.

39. Tsai KL, Sun YJ, Huang CY, Yang JY, Hung MC, Hsiao CD. Crystal structure of the human FOXO3a-DBD/DNA complex suggests the effects of post-translational modification. Nucleic Acids Res. 2007;35:6984-94.

40. Bouillet P, Zhang LC, Huang DC, Webb GC, Bottema CD, Shore P, et al. Gene structure alternative splicing, and chromosomal localization of pro-apoptotic Bcl-2 relative Bim. Mamm Genome. 2001;12:163-8.

41. Gilley J, Ham J. Evidence for increased complexity in the regulation of Bim expression in sympathetic neurons: involvement of novel transcriptional and translational mechanisms. DNA Cell Biol. 2005;24:563-73.

42. Gilley J, Coffer PJ, Ham J. FOXO transcription factors directly activate bim gene expression and promote apoptosis in sympathetic neurons. The Journal of cell biology. 2003;162:613-22.

43. Marks P, Rifkind RA, Richon VM, Breslow R, Miller T, Kelly WK. Histone deacetylases and cancer: causes and therapies. Nature reviews Cancer. 2001;1:194-202.

44. Fullgrabe J, Kavanagh E, Joseph B. Histone onco-modifications. Oncogene. 2011;30:3391-403.

45. Wang F, Marshall CB, Li GY, Yamamoto K, Mak TW, Ikura M. Synergistic interplay between promoter recognition and CBP/p300 coactivator recruitment by

FOXO3a. ACS chemical biology. 2009;4:1017-27.

46. Egle A, Harris AW, Bouillet P, Cory S. Bim is a suppressor of Myc-induced mouse B cell leukemia. Proc Natl Acad Sci U S A. 2004;101:6164-9.

47. Paschos K, Smith P, Anderton E, Middeldorp JM, White RE, Allday MJ. Epstein-barr virus latency in B cells leads to epigenetic repression and CpG methylation of the tumour suppressor gene Bim. PLoS pathogens. 2009;5:e1000492.

48. Hu MC, Lee DF, Xia W, Golfman LS, Ou-Yang F, Yang JY, et al. IkappaB kinase promotes tumorigenesis through inhibition of forkhead FOXO3a. Cell. 2004;117:225-37.

Table 1

Gene	Fold change	Gene ontology
API5	2.18	anti-apoptosis
BCL2L11 (Bim)	-9.93	induction of apoptosis
CARD11	2.87	regulation of apoptosis
CASP1	2.97	apoptosis
CD28	4.60	positive regulation of anti-apoptosis
COP1	9.41	regulation of apoptosis
DEDD2	2.01	induction of apoptosis via death domain receptors
DYRK2	2.16	induction of apoptosis
GZMB	-5.90	apoptosis
HIPK2	2.19	induction of apoptosis by intracellular signals
NLRP1	3.08	induction of apoptosis
PI3KR2	-2.68	negative regulation of anti-apoptosis
PLEKHF1	2.99	induction of apoptosis
PRDX2	-2.10	anti-apoptosis
PRF1	3.95	virus-infected cell apoptosis
RFFL	2.20	apoptosis
SPHK1	-4.26	anti-apoptosis
TNFRSF9	-2.61	induction of apoptosis
TP53INP1	2.32	apoptosis
VEGFA	-6.96	negative regulation of apoptosis

Figure Legends

Figure 1. HBZ suppresses the transcription of the *Bim* and *FasL* genes and consequently stimulation-induced apoptosis. A, Comparison of the *Bim* mRNA expression in the Jurkat-control, Jurkat-HBZ, CEM-control, and CEM-HBZ cells with or without PMA/Io stimulation by real time PCR. B, Jurkat-control and Jurkat-HBZ were stimulated with PMA/Io for 9h and stained with Annexin V. Percentage of apoptotic cells was determined by a flow cytometry. C, Jurkat-control and Jurkat-HBZ were treated with Fas blocking antibody for 30 min and then stimulated with PMA/Io for 9h. Percentages of apoptotic cells were monitored by flow cytometry. D, Comparison of the *FasL* mRNA transcription in the Jurkat-control, Jurkat-HBZ, CEM-control, and CEM-HBZ cells with or without PMA/Io stimulation by real time PCR. Error bars indicate standard deviation. Statistical differences are calculated by Student's *t*-test.

Figure 2. HBZ attenuates function of Foxo3a by physical interaction. A, Jurkat cells were transfected with FoxO3aAAA, a constitutively active form, expressing vector by using Neon with or without HBZ or its mutants. 24h after transfection, cells were stained with Annexin V and analyzed by a flow cytometry (n = 3). B, Jurkat cells were transfected with FoxO3aAAA expressing vector together with HBZ or its mutants by using Neon. Cells were stained with Annexin V and analyzed by flow cytometry (n = 3). Data are representative of three independent experiments. C, Reporter construct

containing the 6 x DBE and FoxO3aAAA expressing vector was transiently transfected with or without HBZ into Jurkat cells in the presence of Z-VAD-FMK and luciferase activities were measured. D, 293T cells were transfected with 6xDBE-Luc construct, and Flag-tagged FoxO3aAAA expression vector together with or without HBZ expression vector. Cells were immunoprecipitated with anti-Flag antibody and quantified by real-time PCR. Three independent ChIP experiments have been done and a representative data is shown. Error bars indicate experimental variation. E and F, The expression vectors of the indicated proteins were co-transfected into 293T cells, and their interactions were analyzed by immunoprecipitation assay. Data are representative of three independent experiments. Statistical differences are calculated by Student's *t*-test.

Figure 3. HBZ interferes normal localization of FoxO3a by forming ternary complex with FoxO3a and 14-3-3. 293FT cells were transfected with FoxO3aWT-Flag together with or without mycHis-HBZ. FoxO3a was detected using anti-Flag-biotin and secondary Streptavidin-Alexa 488 (A), and p-FoxO3a was detected using anti-p-FoxO3a (ser253) and secondary anti-rabbit IgG-Alexa 488 antibody (B). DAPI was used to counterstain the nucleus. C, 293FT cells were transfected with HA-tagged FoxO3aWT together with or without Flag-tagged HBZ. Cytoplasmatic and nuclear fraction were extracted and p-FoxO3a was detected by western-blotting. D, Endogenous localizations of p-FoxO3a (ser253) in HeLa and MT-1 cells were examined using anti-p-FoxO3a. E, The interactions among HBZ, FoxO3a and 14-3-3 were analyzed by

immunoprecipitation.

Figure 4. Bim expression is also suppressed in ATL cell lines and ATL cases. Comparison of the *Bim* mRNA expression in non-ATL cell lines and ATL cell lines with or without PMA/Io stimulation (A) and in PBMCs and PHA-blasts from healthy donor samples and fresh ATL samples (B) by real time PCR. C, Comparison of the *Bim* mRNA expression in healthy donor sample and ATL fresh sample with or without PMA/Io stimulation.

Figure 5. Epigenetic status of the promoter regions of the *Bim* gene. A- C, The presented diagram shows the fold difference of acetylated histone H3, acetylated histone H4, trimethylated H3K4, dimethylated H3K9, or trimethylated H3K27 where the data from Jurkat cells was arbitrarily set as 1.0. D, Quantitative ChIP assay using RNA polymerase II (Pol II) antibody in Jurkat, MT-1and TL-Om1 cells. E, 293T cells were transfected with HA-tagged FoxO3a expression vector together with or without HBZ expression vector. Cells were immunoprecipitated with anti-HA antibody and DNA binding ability at promoter 2 was quantified by real-time PCR. F, The presented diagram shows the fold difference of acetylated histone H3 in MT-1 cells, which were treated with or without 0.4 mM TSA for 15h. The data from MT-1 cells without TSA treatment was arbitrarily set as 1.0. G and H, MT-1 cells were treated with 0.4 mM TSA for 15h and *Bim* expression level was analyzed by qRT-PCR and flow cytometry. I, The presented diagram shows the fold difference of acetylated histone H3 in the Bim

promoter in the Jurkat-control and Jurkat-HBZ cells 9h after the stimulation with PMA/Io. J, HBZ transcript in shRNA transfectant of MT-1 was quantified by real-time PCR. K, Comparison of the *Bim* mRNA expression in control MT-1 cells and HBZ-KD MT-1 cells. Error bars indicate experimental variation. The data shown are representative of two or three independent experiments. Statistical differences are calculated by Student's *t*-test.

Table 1. Apoptosis-associated genes that are up- or downregulated by HBZ. A list of apoptosis-associated genes that were down-regulated or up-regulated (by > 2-fold) in stimulated Jurkat-HBZ cells identified by microarray analysis.

Figure 1

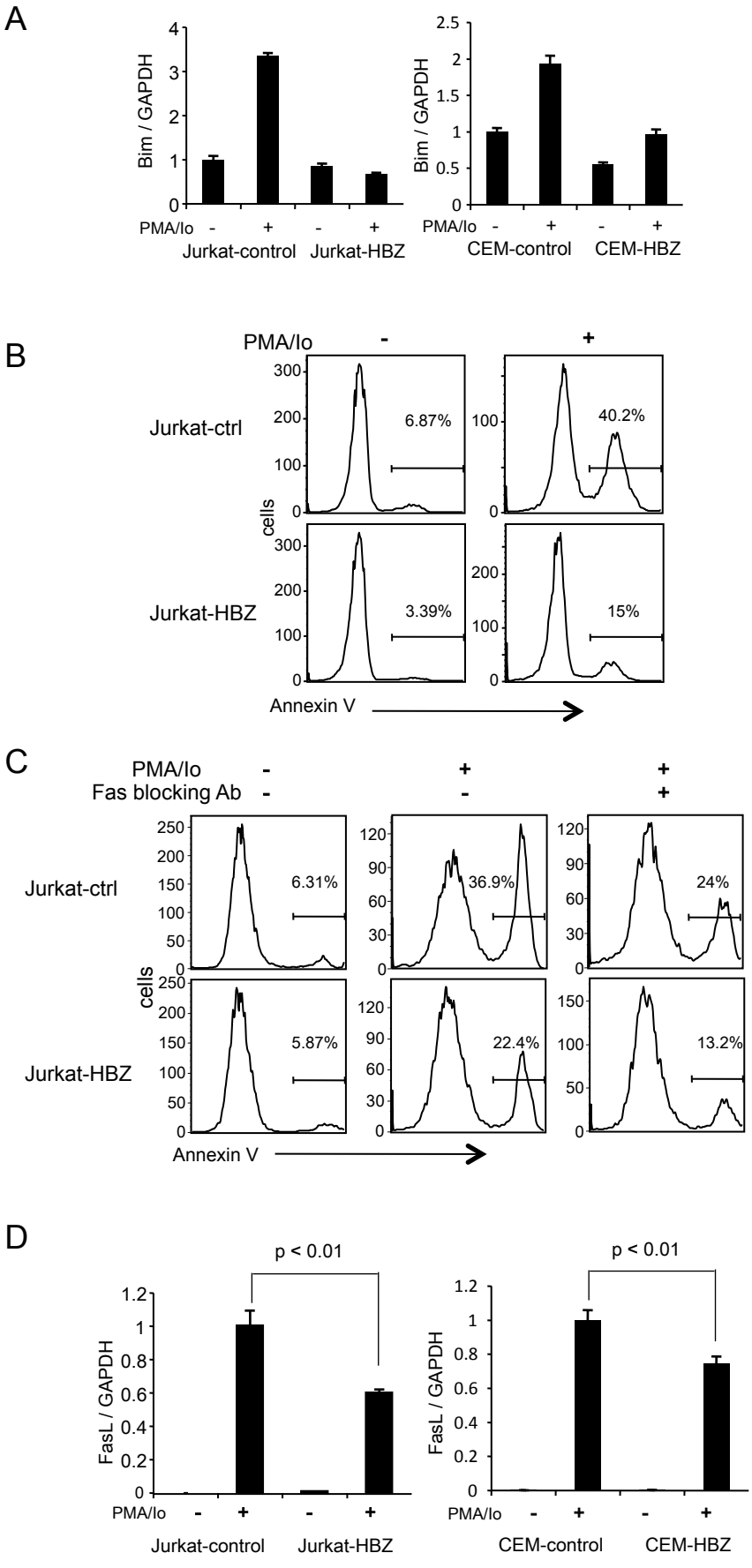
A
Bim / GAPDH
PMA/Io
Jurkat-control
Jurkat-HBZ
CEM-control
CEM-HBZ
B
PMA/Io
Jurkat-ctrl
Jurkat-HBZ
6.87%
40.2%
3.39%
15%
cells
Annexin V
C
PMA/Io
Fas blocking Ab
Jurkat-ctrl
Jurkat-HBZ
6.31%
36.9%
24%
5.87%
22.4%
13.2%
cells
Annexin V
D
p < 0.01
FasL / GAPDH
PMA/Io
Jurkat-control
Jurkat-HBZ
CEM-control
CEM-HBZ

Figure 2

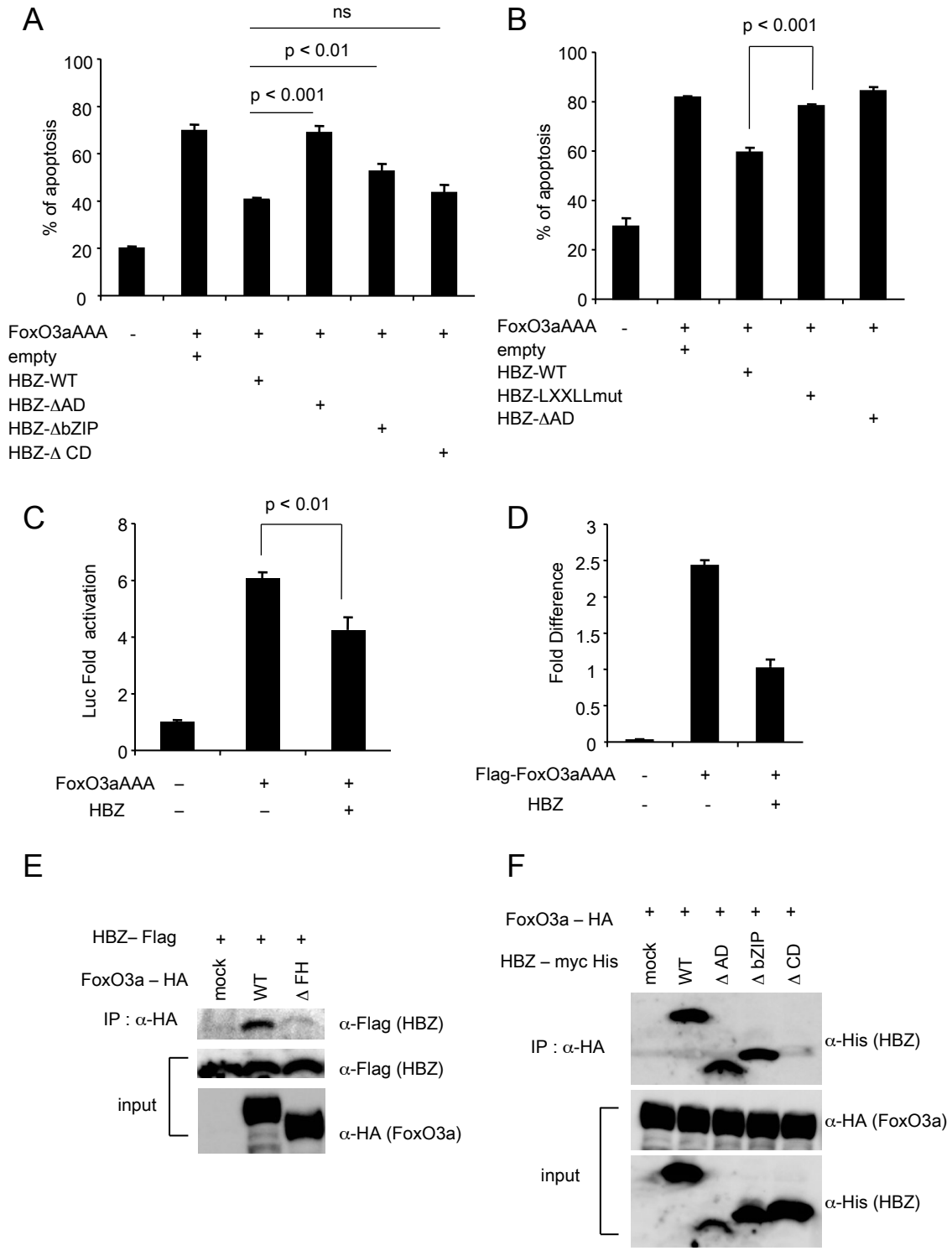
A
ns
p < 0.01
p < 0.001
% of apoptosis
100
80
60
40
20
0
FoxO3aAAA - + + + + +
empty +
HBZ-WT +
HBZ-ΔAD +
HBZ-ΔbZIP +
HBZ-Δ CD +
B
p < 0.001
% of apoptosis
100
80
60
40
20
0
FoxO3aAAA - + + + +
empty +
HBZ-WT +
HBZ-LXXLLmut +
HBZ-ΔAD +
C
p < 0.01
Luc Fold activation
8
6
4
2
0
FoxO3aAAA – + +
HBZ – – +
D
Fold Difference
3
2.5
2
1.5
1
0.5
0
Flag-FoxO3aAAA - + +
HBZ - - +
E
HBZ– Flag + + +
FoxO3a – HA mock WT Δ FH
IP : α-HA
α-Flag (HBZ)
α-Flag (HBZ)
input
α-HA (FoxO3a)
F
FoxO3a – HA + + + + +
HBZ – myc His mock WT Δ AD Δ bZIP Δ CD
IP : α-HA
α-His (HBZ)
α-HA (FoxO3a)
input
α-His (HBZ)

Figure 3

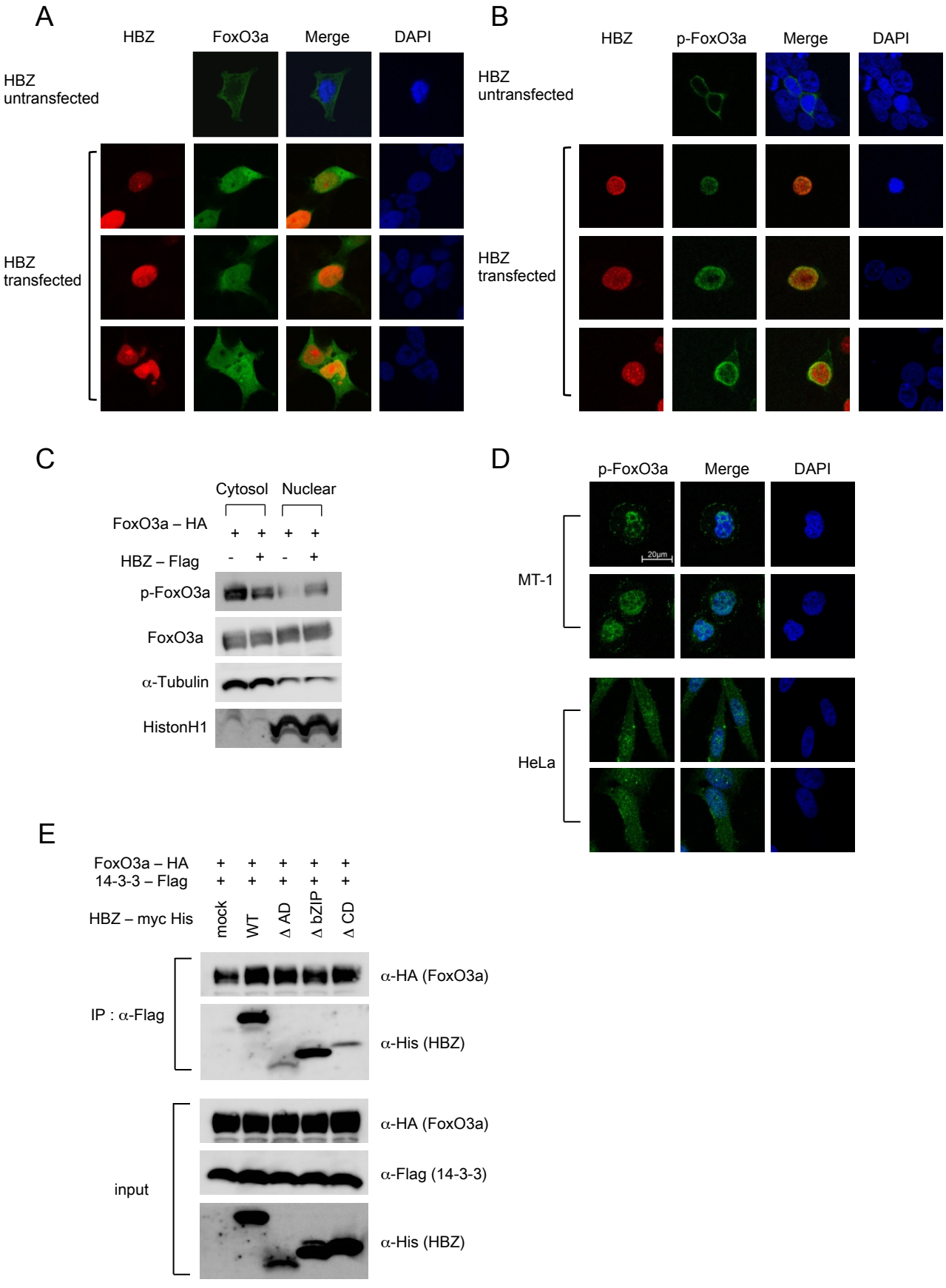
A
HBZ
FoxO3a
Merge
DAPI
HBZ untransfected
HBZ transfected
B
HBZ
p-FoxO3a
Merge
DAPI
HBZ untransfected
HBZ transfected
C
Cytosol
Nuclear
FoxO3a – HA
+ + + +
HBZ – Flag
- + - +
p-FoxO3a
FoxO3a
α-Tubulin
HistonH1
D
p-FoxO3a
Merge
DAPI
20μm
MT-1
HeLa
E
FoxO3a – HA + + + + +
14-3-3 – Flag + + + + +
HBZ – myc His
mock
WT
Δ AD
Δ bZIP
Δ CD
IP : α-Flag
α-HA (FoxO3a)
α-His (HBZ)
input
α-HA (FoxO3a)
α-Flag (14-3-3)
α-His (HBZ)

Figure 4

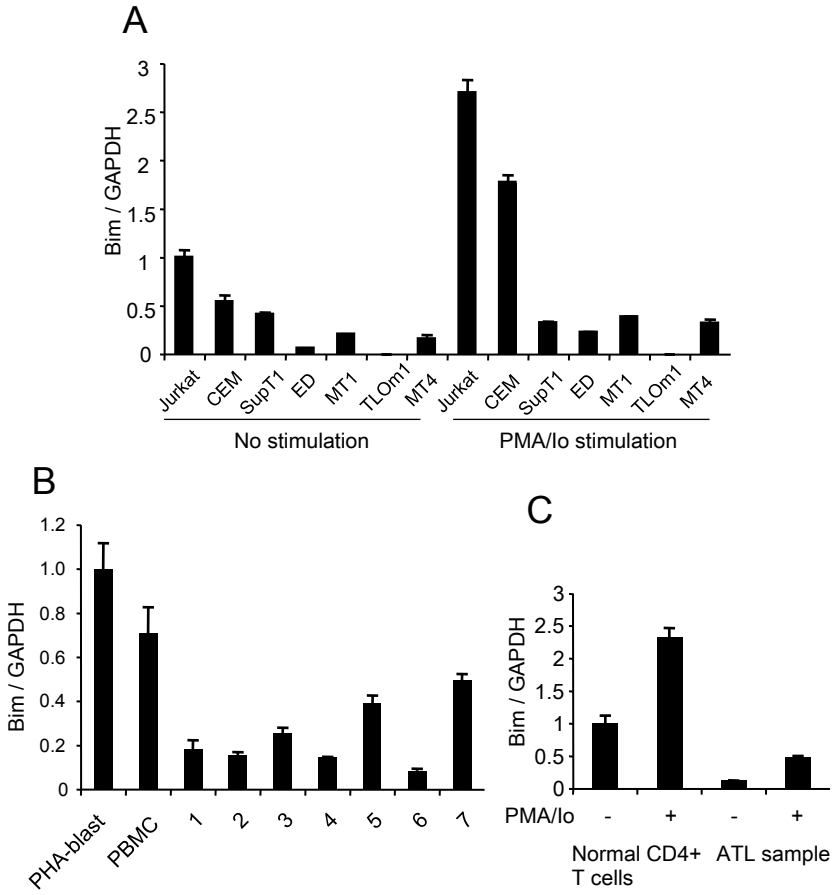
A
Bim / GAPDH
3
2.5
2
1.5
1
0.5
0
Jurkat
CEM
SupT1
ED
MT1
TLOm1
MT4
Jurkat
CEM
SupT1
ED
MT1
TLOm1
MT4
No stimulation
PMA/Io stimulation
B
Bim / GAPDH
1.2
1.0
0.8
0.6
0.4
0.2
0
PHA-blast
PBMC
1
2
3
4
5
6
7
C
Bim / GAPDH
3
2.5
2
1.5
1
0.5
0
PMA/Io
-
+
-
+
Normal CD4+ T cells
ATL sample

Figure 5

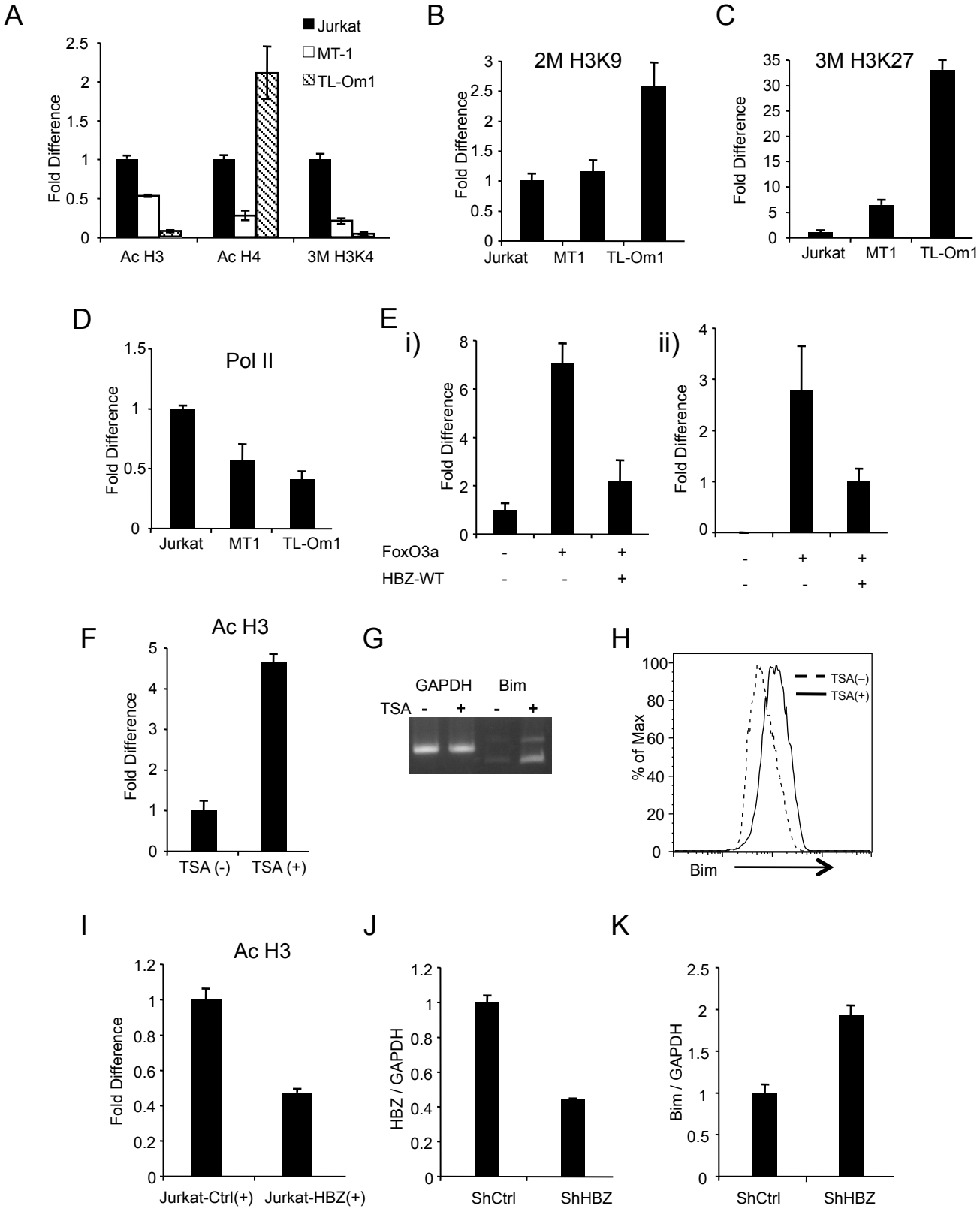
A
Jurkat
MT-1
TL-Om1
Fold Difference
Ac H3
Ac H4
3M H3K4
B
2M H3K9
Fold Difference
Jurkat
MT1
TL-Om1
C
3M H3K27
Fold Difference
Jurkat
MT1
TL-Om1
D
Pol II
Fold Difference
Jurkat
MT1
TL-Om1
E
i)
ii)
Fold Difference
FoxO3a
HBZ-WT
F
Ac H3
Fold Difference
TSA (-)
TSA (+)
G
GAPDH
Bim
TSA
H
% of Max
TSA(–)
TSA(+)
Bim
I
Ac H3
Fold Difference
Jurkat-Ctrl(+)
Jurkat-HBZ(+)
J
HBZ / GAPDH
ShCtrl
ShHBZ
K
Bim / GAPDH
ShCtrl
ShHBZ